Ultrasonics Sonochemistry 111 (2024) 107138

Contents lists available at ScienceDirect

Ultrasonics Sonochemistry

journal homepage: www.elsevier.com/locate/ultson

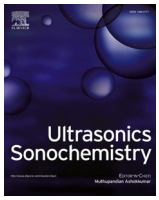

Circulation process of methyl ester production from pretreated sludge palm oil using CaO/ABS catalytic static mixer coupled with an ultrasonic clamp

Kritsakon Pongraktham, Krit Somnuk *

Department of Mechanical and Mechatronics Engineering, Faculty of Engineering, Prince of Songkla University, Hat Yai, Songkhla 90110, Thailand

ARTICLE INFO

Keywords:
3D printing
Biodiesel production
Catalytic static mixer
Heterogeneous catalyst
Sludge palm oil
Ultrasound

ABSTRACT

This study investigates the potential of fused deposition modeling (FDM) three-dimensional (3D) printing techniques for manufacturing catalytic static mixers during biodiesel synthesis. The printed catalytic mixing elements comprises acrylonitrile butadiene styrene (ABS) plastic with 15 wt% calcium oxide (CaO) as a solid catalyst. When the reactants flowed through the CaO/ABS mixing device, the blending and acceleration processes were both significantly impacted. Moreover, their characteristics, performance in biodiesel production, reusability, and economy were analyzed. The effects of methanol to oil (M:O) molar ratio, circulation time, and sonication time on methyl ester (ME) purity were also examined. The results showed that CaO crystals were distributed on the CaO/ABS mixer's surface, which is crucial for catalytic purposes. During circulation process of ME from pretreated sludge palm oil (PSPO), catalytic static mixer (CSM) and CSM coupled with ultrasound (CSM/US) reactors were employed. The full ultrasonic power of CSM/US reactor of 16 × 400 W (total 6400 W) was operated at 20 kHz frequency. Moreover, the continuous and pulse ultrasonic modes of CSM/US reactor were compared to determine the ME purity and electricity consumption for ME production. For the CSM reactor, 12:1 M:O molar ratio and 8.5 h circulation time were recommended to realize 94.2 wt% ME purity. For the CSM/US reactor, 12:1 M:O molar ratio and 2.25 h circulation time were recommended to achieve 96.5 wt% ME purity. Under the pulsed mode operation, ME purity of 95.09 wt% was achieved, with a reduction in electricity consumption by approximately 37.6 % compared to continuous mode operation. Furthermore, the CaO/ABS catalytic static mixer was determined to be reusable for up to three cycles in both CSM and CSM/US reactors. Thus, CaO/ABS catalytic static mixers assure high purity ME production through FDM 3D printing technology with a CaO solid catalyst.

1. Introduction

Biodiesel can be produced through several renewable sources, including vegetable oils, fats, and waste oil. In Thailand, crude palm oil (CPO) is employed as the primary feedstock during commercial biodiesel production. However, palm oil is favorably employed by food manufacturers due to its advantageous nutritional values. Thus, Thailand's renewable energy program is exploring feedstocks that are not used in food production [1]. To address these issues, non-edible oils or waste raw materials, including camelina, jatropha, sludge, and waste cooking oils, have been used as second generation feedstocks for biodiesel production [2]. A waste material discharged from palm oil mill plantations is sludge palm oil (SPO). Generally, microorganisms utilize the organic matter in palm oil mill effluence (POME) in the absence of oxygen [3]. However, the high oil and fat content of POME could result in the formation of floating scum layers, hindering the digestion process and reducing the gas production efficiency [4]. Hence, the excessive SPO floating fat needs to be removed from the top layer of the POME settling pond [5]. Therefore, SPO could be converted to renewable energy through biodiesel production [3,6]. However, the high free fatty acid (FFA) level of over 1 wt% of feedstocks makes them unsuitable for single-stage biodiesel production via transesterification. During the reaction, the base catalysts could react with the FFA in oil to form soap, affording a lower biodiesel yield. To reduce the FFA in oil raw materials, the FFA needs to be converted into an ester via an esterification process with an acid catalyst, yielding pretreated oil [3,6]. To obtain a high purity ester, a transesterification reaction with a base catalyst is necessitated, which is called the two-stage biodiesel production process [7]. Typically, homogeneous base catalysts are primarily employed during the commercial production of biodiesel. However, the use of

* Corresponding author.
E-mail address: krit.s@psu.ac.th (K. Somnuk).

https://doi.org/10.1016/j.ultsonch.2024.107138
Received 27 June 2024; Received in revised form 24 October 2024; Accepted 29 October 2024
Available online 30 October 2024

homogeneous catalysts has several limitations, including lack of catalyst recovery and reusability, requirement of extensive biodiesel washing, environmental impact, and corrosive problems [8]. To overcome these limitations, the use of heterogeneous catalysts for biodiesel production has been proposed, as they offer better catalyst separation and recovery, minimize waste generation, and have less environmental concerns, leading to cost savings and clean and sustainable biodiesel manufacturing [9].

Heterogeneous base catalysts, such as alkaline earth and alkali metal, transition metal, boron group, and mixed metal catalysts, have been employed in several studies for accelerating transesterification reactions during biodiesel production [10]. The calcium oxide (CaO) solid catalyst has been found to be particularly effective for transesterification reactions. It not only is cost-effective and easy to handle but also has low toxicity levels and reusability [11]. Goli *et al.* (2019) [12] reported the advantages of using a CaO solid catalyst in biodiesel synthesis. They conducted the transesterification reaction of soybean oil using a CaO solid catalyst synthesized from chicken eggshell waste. They experimentally observed that the highest yield of biodiesel of 93 % was obtained under the optimized conditions of 10:1 methanol to oil (M:O) molar ratio, 7 wt% catalyst content, 3 h reaction time, and 57.5 ℃ reaction temperature. However, the biodiesel yield decreased to 75 % after the fifth cycle, indicating that the reaction efficiency decreased with increasing number of reaction cycles [12].

Our previous study [6] conducted a double-step FFA reduction process of SPO using a hydrodynamic cavitation reactor to reduce the 89 wt % initial FFA content to less than 1 wt%. The results showed that the first-step esterification process required 60.8 vol% methanol content, 7.2 vol% sulfuric acid content, 5.0 mm hole diameter, 6.1 mm hole depth, and 3000 rpm rotor speed. Consequently, the FFA content decreased to 36.69 wt% in the actual experiment. Further a second-step esterification process was required to convert the remaining FFA content, yielding a pretreated oil with high purity. In a subsequent experiment, final FFA content of 0.94 wt% was realized in pretreated sludge palm oil (PSPO) under 44.5 vol% methanol content, 3.0 vol% sulfuric acid content, 4.6 mm hole diameter, 5.8 mm hole depth, and 3000 rpm rotor speed. However, the amounts of triglyceride (TG), diglyceride (DG), and monoglyceride (MG) remaining in PSPO were 6.9, 2.6, and 0.3 wt%, respectively. A base-catalyzed transesterification process was employed to further convert the residue glycerides in PSPO into methyl ester (ME) [6]. Thus, this study employs a CaO solid catalyst with acryliconitrile butadiene styrene (ABS) filaments to form a catalytic reactor via three-dimensional (3D) printing.

For the inline mixing device for biodiesel production, static mixers are a highly efficient and cost-effective reactor technology that operate without using any moving parts [13]. Owing to their compact design and minimal space requirements, static mixers are an attractive option for many applications [14]. They are also an effective reactor design for biodiesel production as they enable an even distribution and mixing of glycerides and alcohol, providing an efficient reaction rate and high purity products [15]. In this study, the CaO catalyst was mixed with ABS plastic to extrude catalytic filaments constituting ABS plastic and CaO heterogeneous catalysts [16]. Then, the catalytic mixing elements were fabricated via 3D printing. The conversion of remaining glycerides to biodiesel with methanol can be accelerated using a CaO/ABS catalytic static mixer (CSM). To our knowledge, no study has explored combining ABS and the CaO catalyst and then employing them to 3D print a mixer for biodiesel production. Most studies have focused on applying various coatings, including as Cu, Ni, Pd, Pt, Au, and photocatalyst, on various 3D-printed base models through electroplating or cold spray methods [17,18]. Díez *et al.* (2018) [17] investigated the effectiveness of stainless-steel (SUS304 grade) static mixers coated with TiO_2 in comparison to Fe_2O_3 photocatalysts for removing antibiotic oxytetracycline (OTC) in aqueous solution. They determined that the spray coating technique was more effective for OTC degradation than the dip coating technique. Furthermore, the Fe_2O_3 catalyst exhibited superior results compared to the TiO_2 catalyst: the pseudo-first-order kinetic constant was 79 % higher [17]. Lebl *et al.* (2022) [18] fabricated stainless-steel (SUS316L grade) static mixers coated with Pd/Al_2O_3 via additive manufacturing for continuous flow hydrogenation of nitroaromatics. The mixers demonstrated excellent catalytic performance, superior heat and mass transfer, high stability, and no significant metal leaching. Moreover, their design enables easy scalability, promotes sustainable practices, minimizes waste, maximizes the application of 3D printing, and demonstrates the potential for pharmaceutical applications [18].

In addition to fabricating CaO/ABS mixing elements via 3D printing, this study aims to examine the influence of employing ultrasonic waves with a catalytic static mixer in the transesterification reactions during biodiesel production. Since ultrasound affords higher mixing intensity via acoustic cavitation stemming from the pressure vibration of ultrasonic transducers, its application leads to a shorter reaction time, increased conversion of esters, and shorter separation time for biodiesel and glycerol [19]. In continuous processes, ultrasonic tubular clamp reactors have been reported to enhance the mixing intensity, making them valuable in industrial production processes. Furthermore, Chipurici *et al.* (2019) [20] compared various methods for producing biodiesel from waste materials in terms of efficiency and energy consumption, including ultrasonic, hydrodynamic cavitation, and microwave reactors. They found that ultrasonic clamps exhibited superior efficiency in converting oil to biodiesel [20].

As an application of ultrasound in circulation and continuous biodiesel production processes with heterogeneous catalysts, Malani *et al.* (2017) [21] studied ultrasound-assisted biodiesel synthesis using a Cu_2O heterogeneous catalyst and mixed non-edible oil feedstock. Their results showed that ultrasound improved reaction kinetics, reduced mass transfer barriers, and enhanced process efficiency [21]. There are few studies focusing on integrating ultrasonic and static mixer reactors to accelerate biodiesel production with heterogeneous catalysts. For instance, Poosumas *et al.* (2016) [22] investigated the biodiesel production from refined palm oil using a circulated continuous-flow ultrasonic reactor with packed CaO as a solid base catalyst. The study found that ultrasonic irradiation significantly enhanced the transesterification process by improving mixing and reducing activation energy, leading to higher biodiesel yields. The CaO catalyst also demonstrated good reusability, maintaining high biodiesel yields over three cycles. [22]. Nevertheless, the continuous use of ultrasound raises concerns due to its high energy consumption. To address this, the pulse mode has been used to reduce electricity consumption. The pulse mode is defined by alternating periods of ultrasonic energy application, which can lower energy use. Sharma *et al.* (2020) [19] compared continuous and pulsed ultrasonic modes in biodiesel production with CaO heterogeneous catalysts. They found that pulsed modes required less energy compared to continuous modes, though they resulted in lower biodiesel yields and longer reaction times. But, a continuous mode provided faster reaction time and higher biodiesel yield due to higher mixing intensity from continuous sonication mode [19]. Therefore, the current study utilized the circulation process to produce the biodiesel from PSPO by integrating an ultrasonic clamp reactor and CaO/ABS catalytic static mixer.

To our knowledge, no study has investigated the utilization of a catalytic static mixer coupled with an ultrasonic reactor (CSM/US) for converting glycerides to ME via the heterogeneous transesterification reaction. Therefore, this current study aimed to observe the ME purity obtained with the CSM and CSM/US reactors. Two independent factors were varied to determine the ME purity, i.e., circulation time and M:O molar ratio, under 5 L/h flow rate while circulating the mixtures through the reactor. Furthermore, the surface morphology, characteristics, reusability of the CaO/ABS catalytic static mixers, and electricity consumption of the two reactors were analyzed. In addition, the electricity and ME purity of biodiesel production were described using the CSM/US reactors in both continuous and pulsed ultrasonic modes.

Table 1
Physicochemical properties of SPO, PSPO, and biodiesel with biodiesel standards.

Property	Analysis method	Unit	Biodiesel standards			Results		
			US [25]	EU [25]	THA [26]	SPO [6]	PSPO [6]	Biodiesel (This study)
Compositions								
ME	TLC/FID	wt%	–	min 96.5	min 96.5	–	89.25	96.51
TG	TLC/FID	wt%	max 0.2	max 0.2	max 0.2	9.80	6.93	1.39
DG	TLC/FID	wt%	–	max 0.2	max 0.2	0.80	2.57	1.46
MG	TLC/FID	wt%	–	max 0.2	max 0.7	0.24	0.30	0.34
FFA	TLC/FID	wt%	–	–	–	89.16	0.94	0.30
Specific gravity	ASTM D1298	–	0.86–0.90[b]	0.86–0.90[b]	0.86–0.90[b]	0.865[c]	0.850[c]	0.887[b]
Viscosity	ASTM D445	cSt	1.9–6.0[d]	3.5–5.0[d]	3.5–5.0[d]	3.89[c]	5.36[d]	6.44[d]
Cloud point	ASTM D2500	℃	–	–	–	–	13	13
Pour point	ASTM D97	℃	–	–	–	42	11	11
Acid value	ASTM D664	mg KOH/g	max 0.5	max 0.5	max 0.5	197.7	1.8	1.4
Yield of biodiesel	Calculation[a]	wt%	–	–	–	–	98.3	86.5

Note: [a] The biodiesel yield was determined by dividing the weight of the biodiesel product (g) by the initial weight of SPO (g), which was 100 wt%.
[b] at 15 ℃.
[c] at 60 ℃.
[d] at 40 ℃.

2. Materials and methods

2.1. Materials

To reduce the high FFA levels in SPO, our previous study employed a double-step esterification process using a hydrodynamic cavitation reactor [6]. The FFA levels were reduced from 89 wt% to less than 1 wt %. Therefore, PSPO, the product of the esterification process, was employed as the raw material herein. The physical properties of PSPO are as follows: 5.36 cSt viscosity at 40 °C, 1.8 mg KOH/g acid value, and 0.850 specific gravity at 60 °C. Table 1 lists the compositions of 6.9 wt% TG, 2.6 wt% DG, 0.3 wt% MG, and 89.3 wt% ME [6]. The commercial-grade methanol with 99.8 % purity was purchased from TOP Solvent Co., Ltd., Thailand. For the base catalyst, CaO was blended with ABS plastic materials to form CaO/ABS catalytic filaments. The ABS plastic pellets (HP171, LG Chem Huizhou Petrochemical, China) and laboratory reagent grade CaO solid catalyst (KemAus, Australia) were purchased from local suppliers. A grinder was utilized to reduce the ABS pellets to a fine powder, which was blended with 15 wt% of the CaO solid catalyst to yield the catalytic filaments using a single-screw extruder. The preparation process and mechanical properties of the various CaO concentrations of catalytic filaments (5, 10, and 15 wt%) are described in our previous paper [16]. Titration was performed to determine the acid value in oil using the analytical grade chemical reagents of isopropyl alcohol, potassium hydroxide, and phenolphthalein as indicators [23]. Analytical grade diethyl ether, hexane, benzene, and formic acid were used to analyze the TG, DG, MG, FFA, and ME compositions in biodiesel using a thin-layer chromatography with flame ionization detection (TLC/FID) analyzer and detector (Iatroscan MK-6s, Mitsubishi Kagaku Latron Inc., Tokyo, Japan) [24].

2.2. Printing CaO/ABS catalytic static mixers

The CaO/ABS catalytic static mixer is the key part of this study. It was manufactured by 3D-printing CaO/ABS catalytic filaments into the shape of a corrugated plate static mixer (CPSM-type) mixing element. During the printing procedure, a 3D computer-aided design (CAD) model of the static mixer was translated into GX-code commands for a 3D printer using FlashPrint slicer software (version 5.8.1, Flashforge, China). A dual-nozzle 3D printer (Creator 3, FlashForge, China) with fused deposition modeling technology was employed. The catalytic static mixers were horizontally built layer by layer until the construction was completed. The printing parameters were maintained at a nozzle temperature of 230 ℃ and printing bed temperature of 105 ℃, which was set slightly higher than the glass transition temperature of the catalytic filament (104 ℃) to ensure good adhesion to the build platform [16,27]. To realize high printing quality, 0.4 mm layer height, 10 mm/s printing speed, 100 % plastic filling density, and a 0.8-mm-diameter nozzle were set. The printed models were carefully packed in vacuum seal bags with silica gel to keep them dry and free of moisture-related damage until testing to ensure their quality. The CPSM-type mixing element was selected to investigate the performance of converting the remaining glycerides to ester during biodiesel production. Fig. 1a depicts the CPSM-type mixing element, which was designed as three "W"-shaped corrugated plates arranged perpendicular to each other and set at a 45° angle to the flow direction [15]. The CPSM mixing element had 2 mm thickness, 13 mm length, and 13 mm diameter. Additionally, the length to diameter ratio was 1.0. The average weight of the mixing components was 0.7 g, with a printing time of ~ 7 min/batch. The CaO/ABS catalytic static mixers were inserted into a stainless-steel pipe with an inner diameter of 13 mm, a length of 1000 mm, and a wall thickness of 3.5 mm (Fig. 1d). The gap between the mixer's outer surface and the

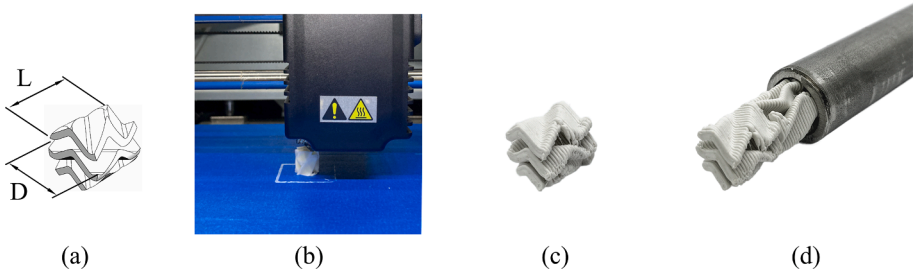

Fig. 1. CaO/ABS catalytic static mixer. (a) CAD model of CPSM type, (b) catalytic static mixer during the printing process, (c) real CaO/ABS catalytic static mixer, and (d) catalytic static mixer in a stainless steel pipe.

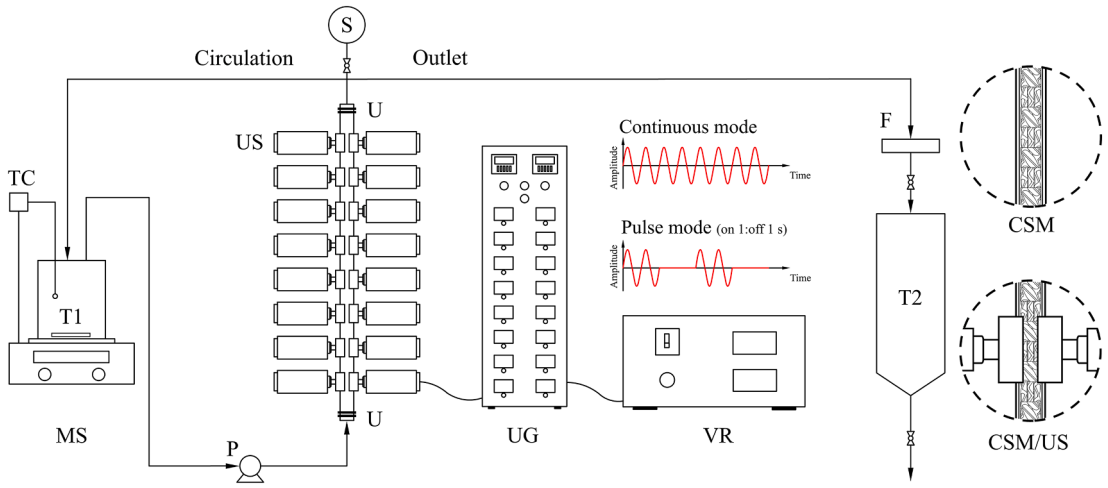

Fig. 2. Schematic of the biodiesel production from PSPO using CaO/ABS catalytic static mixers coupled with ultrasonic clamp reactors. (F: filter, MS: hotplate and magnetic stirrer, P: peristaltic pump, S: sampling port, T1: circulation tank, T2: crude biodiesel tank, TC: temperature control, U: stainless steel union joint, UG: ultrasonic generator, US: ultrasonic tubular clamp, and VR: voltage regulator).

pipe's inner surface was less than 1 mm.

2.3. Analysis methods of CaO/ABS catalytic static mixers

Surface morphology analysis is crucial for determining the structural characteristics of catalytic static mixers and verifying the CaO solid catalyst distribution. Therefore, the surface morphological images of the catalytic static mixers were acquired using a scanning electron microscope (SEM; SU3900, Hitachi, Japan) with backscatter electron image detection mode. The SEM images were captured under an accelerating voltage of 20.0 kV with 30 × and 500 × magnifications. The SEM images comprehensively depicted the CaO solid catalyst/ABS plastic interface structure, highlighting the essential specimen characteristics [28]. To assess the solid catalyst distribution on the 3D-printed catalytic static mixer surface, energy dispersive X-ray spectroscopy (EDS) was performed. Consequently, the calcium elements on the 3D-printed model surface were observed at 1000 × magnification. The material microstructure and surface characteristics for catalyzing purposes were observed [29]. Before the SEM analysis, the samples were coated with gold for 60 s in a vacuum. The surface properties of the CaO/ABS catalytic static mixers were observed using a surface area and porosimetry analyzer (ASAP-2460, Micromeritics, USA) to obtain their specific surface area and pore characteristics. The surface area was determined using the Brunauer, Emmet, and Teller (BET) method. The specific surface area and average pore diameter were obtained through the static volumetric nitrogen gas adsorption technique at − 196.85 ℃ analysis and 70 ℃ degassing temperatures [3]. The functional groups on the catalyst surface were characterized through Fourier transform infrared spectroscopy (FTIR) using a spectrometer (INVENIO-S, Bruker, Germany). The measurements were performed under the 400–4000 cm^{-1} wavenumber range using the KBr pellet method for the CaO powder as a reference and the attenuated total reflection method for the CaO catalytic filaments [30].

2.4. Experimental setup of CSM and CSM/US reactors

Fig. 2 schematically illustrates the experimental setup. Two types of circulation reactors were employed for ME production from PSPO: CSM and CSM/US reactors. The CSM reactor comprised 3D-printed mixing elements inserted into a stainless-steel tube, and it was operated without ultrasound. The stainless-steel tube was SUS304 grade, with an inside diameter of 13 mm, a wall thickness of 3.5 mm, and a length of 1000 mm. In the CSM reactor, the CaO/ABS catalytic mixing component was critical for efficiently mixing and catalyzing the reaction between PSPO and methanol, resulting in ME conversion. Totally, 77 CPSM mixing elements were placed along the 1000-mm tube. The mixtures were supplied by pumping through this static mixer reactor, which operated without any moving parts. For the CSM/US reactor, 16 ultrasonic transducers with ultrasound clamps were mounted on the ultrasonic tube wall. The ultrasonic transducers emitted ultrasonic waves with 400 W ultrasonic power and 20 ± 2 kHz frequency from the wall into the mixture inside the tube, producing a total output of 6400 W (16 × 400 W) when simultaneously operated. The ultrasonic generator (UG) yielded high-frequency ultrasound waves into the ultrasonic transducers. After the CSM and US were entirely installed, mixing and accelerating were simultaneously performed. The dimensionless number used for scaling up reactors, known as the acoustic energy density (AED), was calculated by dividing the ultrasonic power by the volume of the reactants in the tube, as shown in Eq. (1) [24]. Therefore, when operating at the maximum ultrasonic power of 6400 W, the AED was 30.5 W/mL for the maximum mixture volume. Furthermore, the effects of M:O molar ratio, circulation time, and the use of ultrasonic waves on the ME purity were examined during the conversion of PSPO to biodiesel using the CSM and CSM/US reactors. Finally, the effects of continuous and pulse ultrasonic modes were compared to determine the ME purity and electricity consumption for ME production. Consequently, the CSM/US reactors were tested under pulsed ultrasonic conditions, with an ultrasound on-time of 1 s and an ultrasound off-time of 1 s (1 s ON-time/1s OFF-time), in order to save 50 % of the dissipated energy. Meanwhile, a continuous ultrasonic mode without ON/OFF cycles was tested under the same conditions.

$$\mathrm{AED} = \frac{P_{US}}{V_{mixture}} \quad (1)$$

where P_{US} is the power of the ultrasonic reactor (W), and $V_{mixture}$ is the fluid volume of the reactants in the tube (mL).

2.5. Experimental procedure

In all the experiments, the 250 g of PSPO in the PSPO tank (T1) was preheated to 60 ℃ using a hotplate (MS, B S104, RCT Basic, IKA, Germany), as shown in Fig. 2. PSPO was simultaneously stirred at 300 rpm using a digital magnetic stirrer to maintain its temperature with a thermostat-controlled temperature controller (TC, 51 II, Fluke, China). A digital peristaltic pump (P, 323E/D, Watson Marlow, England) was employed to feed the mixture in the tank (T1) at a 5 L/h flow rate to

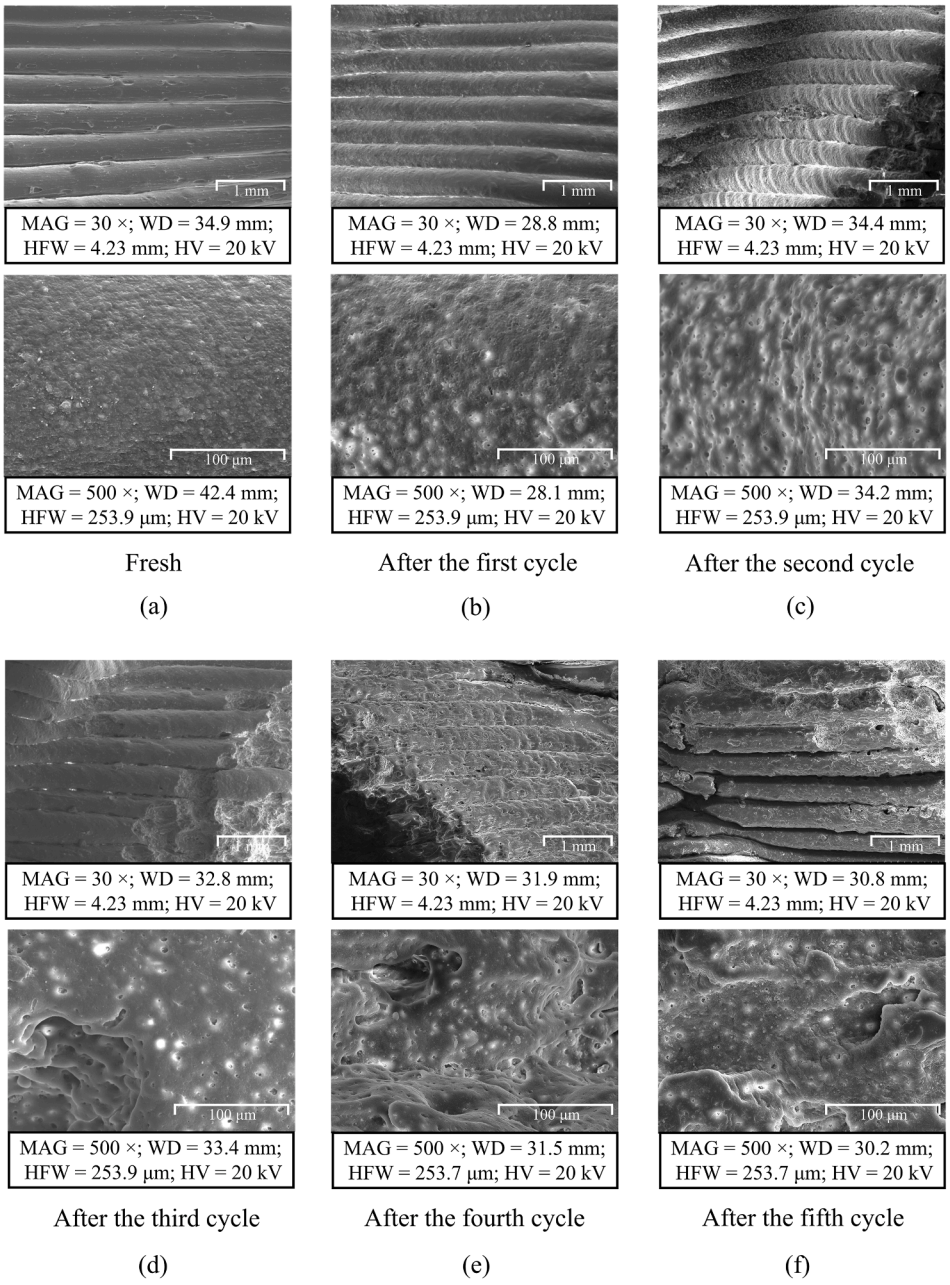

Fig. 3. SEM images of fresh CaO/ABS catalytic static mixer (a), with the catalytic static mixer during the transesterification reactions for the CSM/US reactor after the first (b), second (c), third (d), fourth (e), and fifth (f) reaction cycles at 30 × and 500 × magnifications.

circulate the mixtures passing through the reactor. The M:O molar ratio was varied from 3:1 to 15:1 in methanol increments of 3 mol; the 15 wt% CaO/ABS catalysis concentration of the printed static mixer was fixed at 22.4 wt% with respect to the initial PSPO, and the circulation time of the mixtures was varied from 0 to 3 h for the CSM/US reactor and 0 to 10 h range for the CSM reactor to examine the ME purities during biodiesel production from PSPO. Before commencing the experiment, the required methanol content was poured into the tank (T1), and PSPO was blended for approximately 20 min to obtain a homogenous phase using a stirrer at 300 rpm. When the experiment commenced, the peristaltic pump was turned on so that the PSPO and methanol mixture in tank (T1) was continuously fed into the catalytic static mixer reactor and returned to tank T1, creating a closed loop circulation.

For the CSM reactor, the circulation system continuously operated for 10 h without the assistance of ultrasonic waves. To assess the average ME purity, three 5 mL samples were collected every 30 min from the sampling port (S), which was located at the catalytic static mixer reactor outlet. For the CSM/US reactor, the circulation system was operated with the assistance of ultrasonic waves for 3 h. The PSPO and methanol mixture was fed through the catalytic static mixer reactor via the peristaltic pump in the same closed-loop circulation system as in the CSM reactor. The 16 ultrasonic tubular clamp reactors transmitted ultrasound waves, creating acoustic cavitation in the flowing fluid and enhancing the transesterification reaction. At every 15-min interval, three 5 mL samples were collected at the locations of the sampling ports. The collected sample was rapidly filtered through filter paper (Genuine Whatman No. 1 (11 µm); W. & R. Balston, Kent, UK) and distilled to remove any remaining methanol from the biodiesel through a simple distillation method. All the samples were washed with warm water to dissolve any residual contaminants, including methanol and glycerol byproducts, in the crude biodiesel. The purified biodiesel compositions, including ME, TG, DG, MG, and FFA contents, were assessed via the

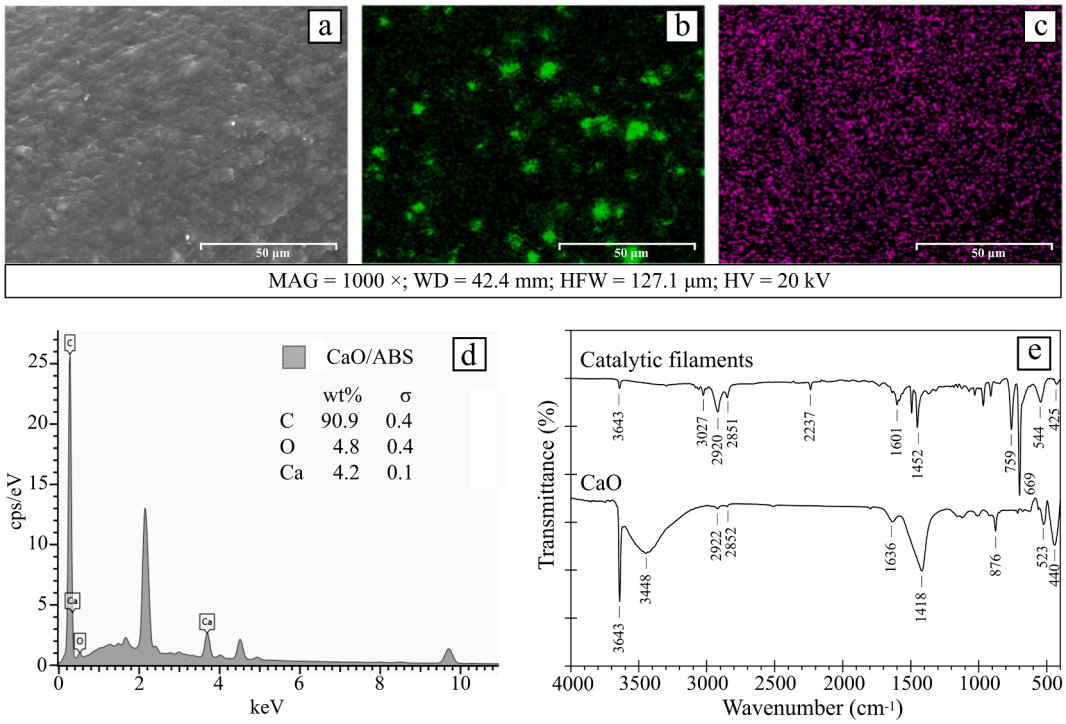

Fig. 4. Characterizations of fresh CaO/ABS catalytic static mixers. (a) surface morphology, (b) calcium element, (c) oxygen element, (d) EDS spectra, and (e) FTIR spectra.

TLC/FID method [24]. Finally, the biodiesel yield was calculated by comparing the weight of the final product relative to 100 wt% of the initial SPO raw material. A tester (MPC-102A, Tanaka, Japan) was employed to measure the pour and cloud points. Additionally, the acid value, viscosity, and density of the biodiesel were measured.

2.6. Reusability study of CaO/ABS catalytic static mixers

The cost of catalytic static mixers could be minimized by reusing them in multiple transesterification processes. To analyze the reusability of the CaO/ABS catalytic static mixers in the transesterification process, both CSM and CSM/US reactors were reused for synthesizing ME from

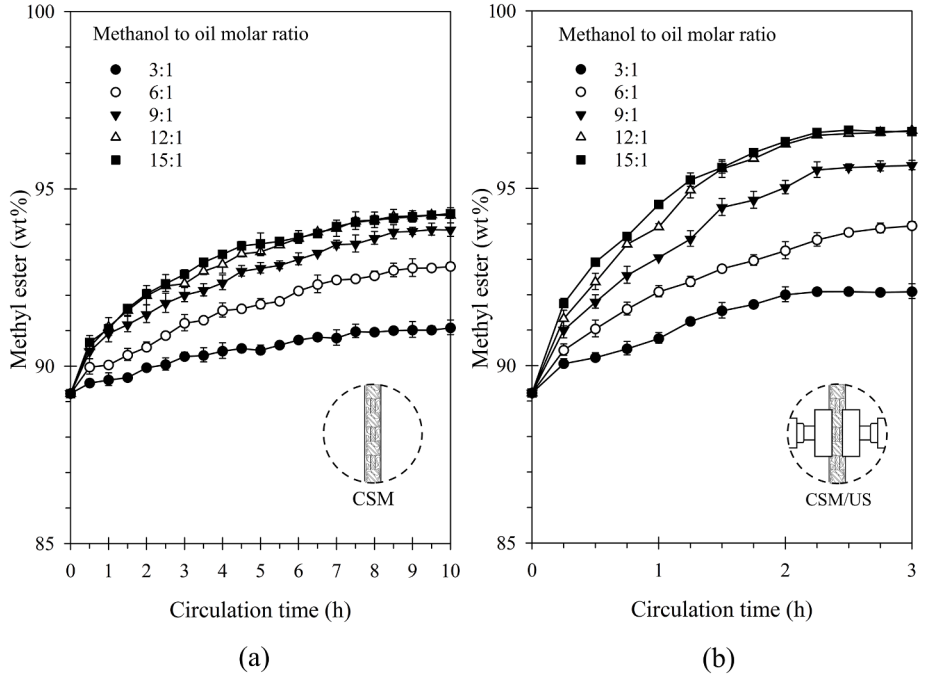

Fig. 5. Comparison of the ME purity of the transesterification process from PSPO under 3:1–15:1 M:O molar ratios and 15 wt% CaO/ABS catalytic static mixer at 5 L/h mixture flow rate using the (a) CSM and (b) CSM/US reactors.

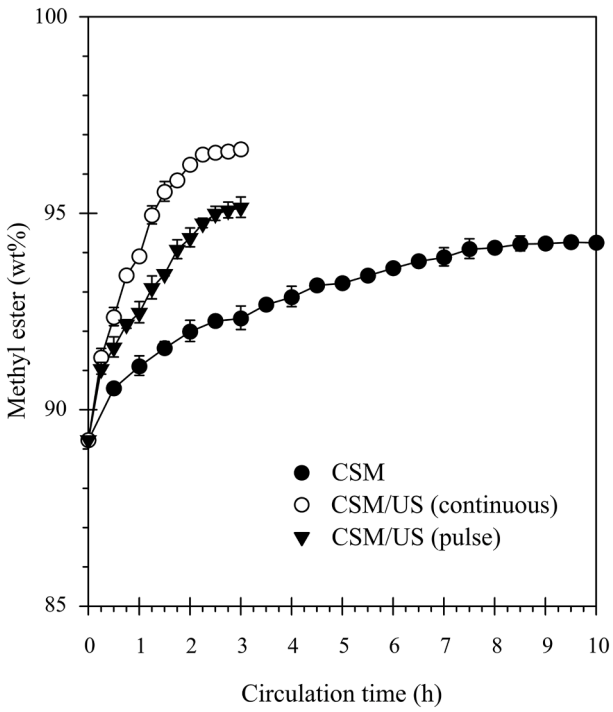

Fig. 6. Comparison of ME purity of transesterification process using CSM, continuous, and pulsed ultrasound for CSM/US reactors under the condition of 12:1 M:O molar ratio.

fresh PSPO in subsequent transesterification circulation processes. Specifically, the catalytic mixing elements of both CSM/US and CSM reactors were repeatedly operated for up to four cycles, and after each process was completed, the catalytic static mixers were regenerated and used for further transesterifications. The recovered catalytic static mixers were carefully cleaned with methanol to remove residual oil films from the surface of the catalytic mixing element before its reuse in the subsequent transesterification cycle. The regeneration process of the CaO/ABS catalytic static mixer follows these steps: (1) fresh methanol was fed into the reactor via a pump to remove any remaining oil films on the surface of the mixing element; (2) the mixing elements were taken out of the reactor; (3) the mixing elements were dried using a hot air oven at 40 ℃ for 12 h to evaporate the residual methanol; (4) the reused catalytic static mixers were kept in a zip-locked vacuum plastic bag to prevent the moisture in the air. To evaluate the reusability of the recovered catalytic static mixer, the ME purities were analyzed using TLC/FID after the circulation process of both CSM and CSM/US reactors. Since this study aimed to examine the ester conversion efficiency under multiple transesterification process, the catalytic static mixer was utilized for five cycles. Its surface was viewed using an SEM, enabling a thorough examination of the surface morphology changes during multiple process cycles.

3. Results and discussion

3.1. Characterizations of CaO/ABS catalytic static mixers

The presence of CaO crystals on the mixer surface is crucial in catalytic processes, as confirmed by SEM/EDS, BET, and FTIR analyses. The SEM imaging provided significant insight into the morphological changes occurring on the catalytic static mixer surface during catalytic reactions. Particularly, the mixing elements of the CSM/US reactor were analyzed using an SEM to monitor the surface damage due to acoustic cavitation. SEM imaging was also utilized to investigate the cause of the reaction drop observed over several cycles by analyzing the morphological changes on the mixing element surfaces [28]. However, the CSM mixing elements were not analyzed with the SEM due to the occurrence of insignificant damage. Fig. 3 depicts the SEM images at 30 × and 500 × magnifications of the fresh and recovered catalytic static mixers after the transesterification reactions of each cycle. The fresh catalytic static mixer exhibited a consistent distribution of white CaO fine crystal spots on the surface, as presented in Fig. 3a. The effects of ultrasonic cavitation on surface damage are discussed in the next section. Moreover, the surface morphology and chemical composition were described using the images taken by the SEM/EDS. Consequently, these SEM/EDS images of the surface of CaO/ABS catalytic static mixers will serve as evidence that the CaO composition disperses on the mixing elements after to the 3D printing process. EDS was conducted to enhance the SEM findings and obtain a better understanding of the element distribution on the fresh catalytic static mixer surface [29]. Fig. 4 illustrates the calcium and oxygen distributions on the fresh catalytic static mixer surface in terms of the surface morphology, calcium element, oxygen element, EDS spectra, and FTIR spectra. The carbon, calcium, and oxygen contents were 90.9, 4.8, and 4.2 wt%, respectively. Localized concentrations of calcium and oxygen were observed on the catalytic static mixer surfaces, corresponding to catalyst deposition or aggregation areas. These regions highlight the role of calcium oxide crystals in catalytic processes and their spatial distribution across the mixer's surface. This is critical for transesterification reactions since CaO compositions on the surface of mixing elements are still distributed for reuse in the next cycle of the transesterification process [31]. Furthermore, the effects of ultrasonic cavitation arising from the ultrasonic clamps of the CSM/US reactor on the catalytic static mixer surface over multiple reaction cycles are discussed in the reusability of catalytic static mixer section.

FTIR analysis provides valuable insights into the chemical structure, bonding, and functional groups on the surface of the CaO/ABS catalytic static mixer, which confirms its catalytic performance in biodiesel production. Fig. 4e presents the FTIR spectra of the CaO/ABS catalytic filament and CaO heterogeneous catalyst. A common peak at 3643 cm^{-1} was observed for both the samples, indicating the presence of O–H stretching vibrations. This was attributed to the CaO catalyst's dehydrating properties, forming calcium hydroxide ($Ca(OH)_2$) [31]. Furthermore, the peaks at 1418 and 876 cm^{-1} were attributed to the stretching and bending modes of C–O in calcium carbonate ($CaCO_3$) stemming from the formation between CaO and carbon dioxide (CO_2) during the extrusion and printing processes [32]. The characteristic peaks associated with vibrations of Ca–O vibrations were observed in the 425–544 cm^{-1} range, verifying the presence of the CaO solid catalyst on their surface [33], which is crucial for the transesterification reaction [31]. The FTIR results were in accordance with Pandit and Fulekar (2019) [31], who examined the use of CaO heterogenous catalyst for transesterification of *Chlorella vulgaris* biomass [31]. These results also align with the XRD from our previous studies and further validate the effectiveness of the CaO catalyst in biodiesel production [16].

BET analysis is crucial for characterizing the physical properties of the CaO/ABS catalytic static mixer, particularly in terms of surface area and pore size. These properties directly influence the catalytic activity, efficiency, and reusability for the production of biodiesel. Based on BET analysis, the specific surface area of the catalytic static mixer was 0.1012 m^2/g, with an average pore diameter of 11.85 nm. Consequently, numerous active sites for catalytic activity were present, promoting efficient mass transfer, blending, and biodiesel production [34]. All results about the CaO catalyst elements occurring on the mixing element surface confirmed that the CaO/ABS mixing element assisted the conversion of glycerides in PSPO to ester in both CSM and CSM/US reactors.

3.2. Biodiesel production using CaO/ABS catalytic static mixers

The ME production of the CSM and CSM/US reactors was compared under 3:1–15:1 M:O molar ratios and 15 wt% CaO/ABS catalytic static mixer, assessing the ME purity. Fig. 5 presents the ME purity versus circulation time for the two reactors.

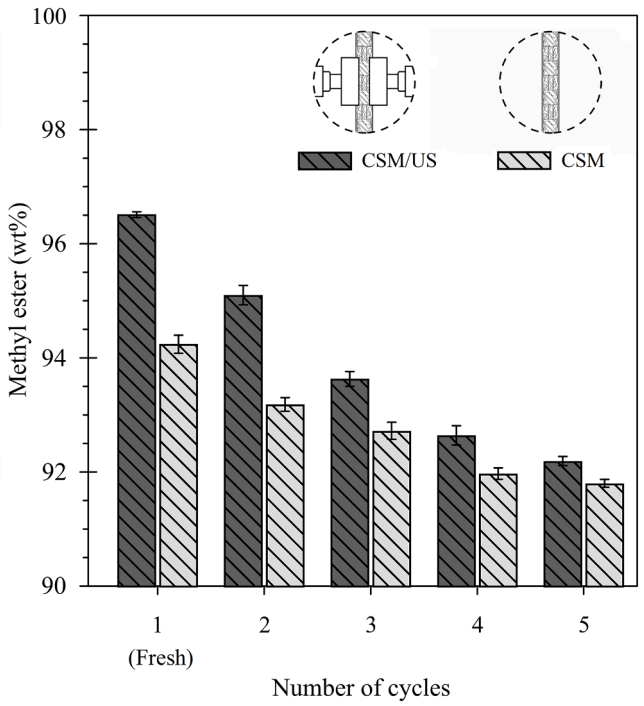

Fig. 7. Comparison of ME purity produced using the CSM and CSM/US reactors across multiple reuse cycles under the recommended conditions.

3.2.1. ME conversion in CSM reactor

The effects of M:O molar ratio on ME purity with 15 wt% CaO/ABS were investigated at ratios of 3:1, 6:1, 9:1, 12:1, and 15:1 for the CSM (Fig. 5a) and CSM/US (Fig. 5b) reactors. All experiments were conducted under 5 L/h mixture flow rate at 60 °C. Fig. 5 compares the ME purities from the transesterification process obtained using CSM and CSM/US reactors. Fig. 5a displays the influences of the M:O molar ratio and circulation time on the ME purity from transesterification process for the CSM reactor. The highest ME purity afforded by the CSM reactor under all the M:O molar ratios within 10 h of circulation time was 94.5 wt% ME. The results indicate that the ME purity slowly increased from 0 to 10 h circulation time under 3:1 M:O molar ratio for the CSM reactor. Furthermore, with 3:1 M:O molar ratio, the ME trend did not reach equilibrium after 10 h of circulation in the CSM reactor. Thus, higher ME purity could be afforded for circulation times exceeding 10 h [28]. Since the transesterification reaction theoretically requires 3 mol of methanol to reach equilibrium, the final biodiesel composition includes unreacted glycerides along with the ME products [35]. Çakırca *et al.* (2018) [36] presented similar results. They obtained a biodiesel yield of 66 % at a 3:1 M:O molar ratio, which was significantly lower than the 90 % biodiesel yield achieved at a 6:1 M:O molar ratio. The M:O molar ratio significantly impacted the conversion efficiency of microalgae oil to biodiesel. Consequently, a high M:O molar ratio is typically employed to enhance biodiesel production [36]. Under 10 h circulation time, the ME purity increased sharply to 92.83, 93.85, 94.27, and 94.32 wt% when the M:O molar ratio was increased to 6:1, 9:1, 12:1, and 15:1, respectively. Furthermore, a higher methanol content is necessary to achieve a higher conversion of glycerides into ME by shifting the equilibrium toward the ester [35]. Moreover, for the CSM reactor, the ME conversions were similar under 12:1 and 15:1 M:O molar ratios. Within 10 h of circulation, the ME purity sharply increased to 94.3 wt%. Under 12:1 M:O molar ratio, the ME purity reached its equilibrium level of 94.24 wt% after 8.5 h in the CSM reactor. However, the biodiesel purity trends did not improve with increasing methanol for the highest M:O molar ratio of 15:1. This is because the catalyst concentration was diluted by the excessive methanol content in the process [37]. Thakur *et al.* (2021) [38] reported similar results. They employed CaO nanocubes synthesized from waste mollusk shells as heterogeneous catalysts for the transesterification process of cottonseed oil. Moreover, they determined that a high M:O molar ratio is necessary for ensuring an entirely completed reaction. The optimal M:O molar ratio of 12:1 resulted in a remarkable increase in the biodiesel yield, reaching up to 95 %. However, excess methanol beyond the optimal ratio reduced the reaction's efficiency. The catalyst efficiency and biodiesel yield decreased when the M:O molar ratio was increased to 15:1 [38]. The maximum ME purity at 10 h circulation time under 3:1, 6:1, 9:1, 12:1, and 15:1 M:O molar ratios was 91.10, 92.83, 93.85, 94.27, and 94.32 wt%, respectively.

3.2.2. ME conversion in CSM/US reactor

Fig. 5b depicts the effects of 0–3 h circulation time and 3:1–15:1 M:O molar ratio on ME purity using a 15 wt% CaO/ABS catalyst for the CSM/US reactor operating at a 5 L/h mixture flow rate and 60 °C. The 16 units of the ultrasonic tubular reactors were constantly operated at 20 kHz with a maximal 400 W power (total 6400 W). As depicted in Fig. 5, the direct comparison of the ME conversions reveals that the CSM/US reactor afforded significantly enhanced ME purities at all molar ratios and circulation times compared to the CSM reactor. Furthermore, extended circulation times resulted in higher ME purities in the CaO solid catalyst systems. Longer duration times enabled a more thorough conversion of glycerides to ME [28]. A product's purity may reach an equilibrium with increasing circulation time. Similarly, after 2.25 h circulation time, the ME purity reached equilibrium regardless of the sonication duration. However, the total manufacturing cost, energy consumption, and reaction times were directly related to the static mixer reactor length when it was operated beyond this circulation time [11]. Ahmed *et al.* (2020) [30] observed a similar trend while optimizing biodiesel production from microalgae using a nano-CaO catalyst synthesized from waste eggshells. They obtained the maximum biodiesel yield of 93.44 % under the optimal reaction time of 180 min. When the reaction time was too low, the transesterification process was not completed, leading to a lower biodiesel yield. This is because the reaction mixture did not have sufficient time to completely react in the heterogeneous catalyst systems. Conversely, when the reaction time exceeded the optimal point, the biodiesel yield decreased due to the possibility of a reverse reaction occurring, which reduced the overall yield [30].

This study examined the effects of the M:O molar ratio on the ME purity. After 3 h circulation time for the CSM/US reactor, ME purity increased to 92.10, 93.95, 95.66, 96.64, and 96.61 wt% as the M:O molar ratio was increased to 3:1, 6:1, 9:1, 12:1, and 15:1, respectively. Particularly, after 3 h of sonication, the 6:1, 9:1, and 12:1 M:O molar ratios resulted in significantly higher ME purities of 64.9 %, 124.9 %, and 159.3 %, respectively, compared to the 3:1 M ratio. This is because the higher methanol content improved the transesterification process, increasing the product's equilibrium level [35]. Moreover, the high methanol content reduced the mixture's viscosity, accelerating methanolysis while enhancing acoustic wave transmission and mass transfer between oil and methanol [39]. However, the ME purity reduced under the 15:1 M:O molar ratio because of catalyst concentration dilution arising from excessive methanol content [35]. These findings are similar to the CSM reactor results. In 2019, Kojima and Takai (2019) [39]

Table 2
Material cost for the CaO/ABS catalytic static mixer during biodiesel production.

Materials	Amount required (g/m of mixer)	Material price (USD/kg)	Material cost (USD/m of mixing element)
ABS plastic[a]	52.2	2.43	0.13
CaO solid catalyst[a]	7.8	47.84	0.37
Total			0.50

Note: [a] The amounts of ABS and CaO solid catalyst were calculated based on 15 wt% CaO loading in ABS plastic.

Table 3
Electricity consumption for forming catalytic static mixers and producing biodiesel.

Lists	Electricity consumption
	(kWh)
Catalytic static mixer forming process	
Catalytic filament extrusion process per meter of catalytic static mixer	0.160
3D printing process per meter of catalytic static mixer	1.100
Total electricity consumption per meter of catalytic static mixer	1.260
Biodiesel production process	
CSM reactor[a]	
Preheating of PSPO to 60 ℃ for 20 min	0.016
Heating to maintain the temperature for 8 h 30 min	0.085
Peristaltic pump at 5 L/h flow rate for 8 h 30 min	0.085
Total electricity consumption for CSM	0.186
CSM/US reactor[b]	
Continuous mode	
Preheating of PSPO to 60 ℃ for 20 min	0.016
Heating to maintain the temperature for 2 h 15 min	0.023
Peristaltic pump at 5 L/h flow rate for 2 h 15 min	0.023
Continuous mode of ultrasonic tubular clamp reactor for 2 h 15 min	2.788
Total electricity consumption for CSM/US	2.848
Pulse mode[c]	
Preheating of PSPO to 60 ℃ for 20 min	0.016
Heating to maintain the temperature for 2 h 45 min	0.028
Peristaltic pump at 5 L/h flow rate for 2 h 45 min	0.028
Pulse mode of ultrasonic tubular clamp reactor for 2 h 45 min	1.705
Total electricity consumption for CSM/US	1.776

Note: The operating conditions were calculated as follows:
[a] For the CSM reactor: 12:1 M:O molar ratio and 8 h 30 min circulation time.
[b] For the CSM/US reactor: 12:1 M:O molar ratio and 2 h 15 min circulation time.
[c] For the pulsed mode: 12:1 M:O molar ratio and 2 h 45 min circulation time.

examined the transesterification of soybean oil and methanol using CaO as a heterogeneous base catalyst. They showed that ultrasonication was 50 % more efficient in reducing reaction time than mechanical stirring, realizing 88 % biodiesel yield within 2.5 h. This improvement stemmed from the intensified cavitation effects, especially at 12:1 M:O molar ratio relative to 6:1 M:O molar ratio. In contrast, under the excessive M:O molar ratio of 18:1, the reaction rate slightly decreased due to the ineffective impingement of soybean oil molecules [39]. In conclusion, the conditions of 12:1 M:O molar ratio and 2.25 h circulation time are recommended for producing biodiesel from PSPO using a CSM/US reactor. Furthermore, compared to the CSM reactor, the CSM/US reactor improves the ME purity by 54.1 %, 31.3 %, 39.3 %, 47.1 %, and 45.2 % under 3:1, 6:1, 9:1, 12:1, and 15:1 M:O molar ratios, respectively, based on the calculations at the end of circulation time of each process. Thus, a higher molar ratio can promote the reaction equilibrium and shorten the circulation time.

3.3. Effects of circulation time on ME purity using CSM, continuous CSM/US, and pulsed CSM/US reactors

The comparison of the CSM, continuous, and pulsed ultrasound for CSM/US reactors in circulation ME production from PSPO was carried out with the recommended condition of 12:1 M:O molar ratio, assessing the ME purity. Fig. 6 shows the ME purity versus circulation time for the various types of reactors. The results for CSM reactor indicate that the ME purity sharply increased at the beginning reaction time in the reactor for 2 h of circulation time. Subsequently, the ME purity gradually increased over the circulation time more than 3 h, and it reached equilibrium level after circulation time of 8.5 h. However, the CSM reactor did not convert the glycerides in PSPO to over 94.5 wt% ME purity, and the 94.27 wt% maximum observed purity of ME was achieved using CSM reactor. To minimize the energy dissipation from the CSM/US reactor during a 3 h circulation time at maximum power of 6400 W, the ME purity was verified during the same reaction time by operating this ultrasonic reactor type in pulse mode. The pulsed CSM/US reactor demonstrated a significant increase in ME purity during the initial reaction time in the ultrasonic reactor, leading to a high level of ME purity after a circulation time of 3 h. The maximum purity of ME was 95.16 wt% achieved within 3 h for pulsed CSM/US reactor. Therefore, 17.7 % improvement in the maximum ME purity was obtained by using the pulsed CSM/US reactor instead of the CSM reactor. For the CSM/US reactor operated under continuous mode, the ME purity profiles in Fig. 6 clearly showed that the continuous CSM/US reactor was superior over the other reactors. The ME conversion sharply increased and gave the highest observed 96.64 wt% purity within 3 h of circulation time. The trend for the continuous mode of the CSM/US reactor demonstrated a sharp increase in the purity of ME after 1 h 15 min circulation time, as the mixture circulated through the reactor and reached equilibrium after 2 h 15 min of circulation time. Therefore, 47.2 %, and 25.0 % improvements in maximum purity of ME were obtained by using the continuous mode of the CSM/US reactor instead of the CSM and pulsed CSM/US reactors, respectively.

In summary, the results showed that the continuous mode of CSM/US reactor was superior over the other reactor types tested. The ester conversion sharply increased and gave the highest observed 96.64 wt% ME purity within 3 h circulation time when the recommended conditions were used. Therefore, combining catalytic mixing elements with the ultrasound clamps was more effective than CSM alone. But, when the energy dissipation from ultrasound was reduced by operating under pulsed conditions with an ultrasound on-time of 1 s and an ultrasound off-time of 1 s to save 50 % of the dissipated energy. This pulsed CSM/US reactor did not reach the glycerides in PSPO to over 95.2 wt% ME purity within the approximately 3 h circulation time. The details of electricity consumption of biodiesel production using CSM, continuous CSM/US, and pulsed CSM/US reactors are described in the next section.

3.4. Compositions, physical properties, and yields of biodiesel product

The characteristics of the biodiesel manufactured using the CSM/US reactor under the recommended conditions of 12:1 M:O molar ratio and 2.25 h circulation time were comprehensively analyzed, including biodiesel compositions, physical properties, and product yields. Table 1 presents the properties of SPO, PSPO, and biodiesel. The compositions in biodiesel produced via CSM/US reactor consisted of 96.51 wt% ME, 1.39 wt% TG, 1.46 wt% DG, 0.34 wt% of MG, and 0.30 wt% of FFA. Compared to the PSPO, the CSM/US reactor increased the biodiesel purity from 89.25 to 96.51 wt%, and produced the MG content of 0.34, which meets Thailand's biodiesel requirement, as listed in Table 1 [26]. However, the remaining 1.39 wt% TG and 1.46 wt% DG in biodiesel are higher than the 0.2 wt% of both TG and DG contents required for biodiesel in Thailand and Europe. Therefore, these TG and DG partial glycerides had to be changed in order to obtain a ME, which is higher than these results. The use of catalyst concentrations in the filaments that exceed 15 wt% CaO/ABS may resolve this issue. Therefore, developing technology to achieve a high concentration of CaO in plastic filaments presents a challenge in terms of converting partial glycerides in oil to meet the biodiesel requirement. The limitation of blending 15 wt% CaO in ABS plastic has been described in section 2.1. Materials. Physical properties of the biodiesel were as follows: 0.887 specific gravity at 15 ℃, 6.44 cSt viscosity at 40 ℃, 13 ℃ cloud point, 11 ℃ pour point, and 1.4 mg KOH/g acid value. The product yield was 88.1 wt%, which was calculated based on the initial raw material of SPO in the first-step esterification process.

3.5. Reusability study of CaO/ABS mixing elements for biodiesel production

To determine the efficiency and performance degradation of catalytic static mixers during multiple biodiesel synthesis cycles, reused CaO/ABS mixing elements were subjected to a circulation transesterification process for biodiesel production from new PSPO. The stability and reduction in catalytic activity were determined by evaluating the ME purities after each cycle. Fig. 7 presents the comparisons of the ME purity afforded by the CSM/US and CSM reactors after five repeated cycles under 12:1 M:O molar ratio, with circulation times of 2.25 h and 8.5 h for the CSM/US and CSM reactors, respectively. Although ME purity decreased for both reactors over time, the CSM/US reactor consistently produced higher ME purities compared to the CSM reactor. For the CSM/US reactor, the ME conversion percentages of biodiesel from the first to the fifth cycle were 67.5 %, 54.4 %, 40.7 %, 31.6 %, and 27.3 %, while the ME purities in biodiesel were 96.51, 95.10, 93.63, 92.64, and 92.19 wt%, respectively, as shown in Fig. 5. In comparison, for the CSM reactor, the ME conversion percentages from the first to the fifth cycle were 46.4 %, 36.5 %, 32.2 %, 25.3 %, and 23.8 %, with corresponding ME purities of 94.24, 93.18, 92.72, 91.97, and 91.80 wt%, respectively. Particularly, the catalytic static mixers became ineffective for biodiesel production when the ME conversion efficiency dropped below 30–40 %, as observed after the third cycle in both reactors. This indicates that the catalytic activity was significantly reduced, and the reactors could no longer perform efficiently for further cycles [40]. Clearly, the reused catalytic mixers from the CSM/US reactor can be used for producing biodiesel from PSPO. However, the improvement in the ME conversion efficiency could decrease by approximately 15 wt% compared to a reaction using new mixing elements. Therefore, the loss of catalytic activity and durability need to be considered when limiting the number of times catalytic static mixers are reused. Particularly, after the third cycle of the CSM/US reactors, damage was observed on the catalytic static mixer surfaces, as shown in Fig. 3. Furthermore, the high intensity of ultrasound waves caused methanol to break down into smaller droplets, thereby increasing the ME purity due to the increase in surface area [41]. However, this phenomenon also damaged the mixer's surface due to acoustic cavitation [42]. Hence, the effectiveness and efficiency of the transesterification reaction can significantly decrease with the catalytic activity over multiple cycles [43]. The mixing elements could be reused for more cycles when the CaO percentage in ABS plastic is increased beyond 15 wt %. Therefore, developing technology to yield a high catalyst concentration in plastic filaments poses a challenge to the strength of the printed model, particularly when the catalyst concentration in the filaments exceeds 15 wt% [16].

3.6. Electricity consumption and cost evaluation

3.6.1. Electricity consumption and cost evaluation of catalytic filament extrusion

This section assesses the electricity consumption for three processes: catalytic filament extrusion, 3D printing, and biodiesel production processes. The overall electricity consumption of the processes was monitored using a digital power analyzer (DM-730, Digicon), as detailed in Tables 2 and Table 3. The costs associated with the manufacturing of the catalytic static mixer were divided into two primary processes: catalytic filament extrusion and 3D printing processes. As listed in Table 2, the average material cost for producing a 1-m-long CaO/ABS static mixer with 15 wt% CaO loading was 0.50 USD, including costs of 0.13 USD for the ABS plastic and 0.37 USD for the CaO solid catalyst, based on the use of 60 g of catalytic filament to fabricate 77 pieces of the mixing elements. The average electricity consumption for forming a 1-m-long catalytic static mixer was 1.260 kWh, with 0.160 and 1.100 kWh attributed to the single screw extruder and 3D printer, respectively, as listed in Table 3.

3.6.2. Electricity evaluations of biodiesel production using the CSM and CSM/US reactors

In terms of the electricity consumption during the circulation process of biodiesel production using the CSM and CSM/US reactors, the sixteen 400 W (full ultrasonic power) ultrasonic clamps were operated at 20 kHz to realize high ME purity from PSPO at 5 L/h flow rate through the reactor. Table 3 lists the electricity consumption for producing biodiesel using the CSM and CSM/US reactors. Specifically, approximately 250 mL of PSPO was preheated and controlled at 60 ℃ for 20 min using a heater to prepare the oil for the transesterification reaction. Subsequently, a peristaltic pump was used to feed PSPO and methanol at a predetermined ratio into the 1000-mm-long circulation reactor. The CSM reactor consumed 0.170 kWh of electricity, while the CSM/US reactor consumed 2.832 kWh at maximum ultrasonic power (excluding the PSPO preheating process). The CSM and CSM/US reactors (Fig. 5) effectively afforded equilibrium levels of ME purity within reaction times of 8 h 30 min and 2 h 15 min, respectively, and their total electricity consumptions were 0.19 and 2.85 kWh, respectively. The average energy consumptions during circulation biodiesel production at 5 L/h by the CSM and CSM/US reactors were 0.63 and 9.68 kWh/L of PSPO, respectively. However, in this study, the electricity consumption per liter of oil was relatively high due to the low initial amount of PSPO used (250 g). The small volume of oil resulted in inefficient energy distribution, leading to increased electricity consumption for the process. Future research will aim to improve this issue by increasing the amount of raw material by more than 250 g, thereby reducing electricity consumption per liter of oil. A similar issue was reported by Gupta *et al.* (2015) [44]. The ultrasonic reactor typically requires more energy compared to conventional stirring methods, but they also suggested that large-scale biodiesel production could benefit from enhanced energy efficiency, effective mass transfer, emulsification of the reaction mixture, and enhancement of the rate of transesterification reaction [44].

3.6.3. Electricity evaluation of biodiesel production using the CSM/US reactors under continuous and pulsed ultrasound

A part of this study is to compare the energy consumption and ME purity of biodiesel synthesis utilizing CSM/US reactors operating under the continuous and pulse ultrasonic modes (1 s ON-time/1s OFF-time). The results of ME purity of biodiesel after CSM and CSM/US with continuous and pulse modes under the recommended conditions are shown in Fig. 6. The ME purity in pulse mode sharply increased with longer circulation time, reaching an equilibrium point at 2 h 45 min. The maximum ME purities were found to be 94.24 wt% for CSM, 96.51 wt% for CSM/US in continuous mode, and 95.09 wt% for CSM/US in pulse mode. Thus, the pulsed CSM/US reactor consumed 1.78 kWh/batch of electricity, which was approximately 37.6 % less than the continuous mode. This demonstrates the potential energy savings when using the pulse ultrasonic mode compared to the continuous mode to obtain the high purity of ME. However, a longer reaction time may lead to a higher electricity consumption when operating a pulsed CSM/US reactor to enhance the level of ME purity, which is close to the ME purity obtained from continuous mode. Therefore, the CSM/US in continuous mode was more effective than the pulse mode, which this ultrasonic duty cycle allowed for a longer reaction time and lower excitation. Similar findings were reported by Sharma *et al.* (2020) [19], who studied the ultrasonic-assisted biodiesel production process from waste cotton seed cooking oil using CaO catalyst. The results found that the ultrasonic reactor achieved higher biodiesel yield of 96.16 %. Moreover, the continuous and pulse modes of sonication were compared to investigate the required energy consumption. The results showed that the continuous mode was more effective, achieving over 90 % biodiesel yield within 20 min, while the pulsed mode required 40 min sonication time. They concluded that the continuous sonication mode was more effective than the pulse mode [19].

4. Conclusions

The CaO/ABS catalytic static mixer was integrated with a 16 × 400 W ultrasound clamp reactor that was set to operate at a frequency of 20 kHz. This CSM/US reactor has successfully converted the glycerides in PSPO to high purity of ME using the transesterification reaction. The presence of CaO crystals on the mixer surface, confirmed by SEM/EDS, BET, and FTIR analyses, was crucial for enhancing catalytic activity. Results indicated that a M:O molar ratio of 12:1 and a circulation time of 8.5 h are recommended conditions for the CSM reactor, while a 12:1 M:O molar ratio and circulation time of 2.25 h were effective for the CSM/US reactor. Ultrasonic enhancement significantly reduced circulation time and enhanced ME purity, achieving 96.5 wt% in the CSM/US reactor. The reusability testing confirmed that the mixer maintained over 92 wt% ME purity across three cycles for both types of reactors. The average electricity consumption for the CSM process was 0.19 kWh/batch, while the CSM/US system required 2.85 kWh/batch. Moreover, the CSM, continuous, and pulsed ultrasound for CSM/US reactors were compared. The continuous mode of the CSM/US reactor was superior over the other reactors. Therefore, the proposed CaO/ABS catalytic static mixer created using 3D printing method and integrated with a CaO solid catalyst is promising and affords high ME purity. In future studies, acid catalytic filaments should be employed to reduce the high FFAs in oil with heterogeneous acid catalysts for the esterification process using a 3D printed static mixer.

CRediT authorship contribution statement

Kritsakon Pongraktham: Writing – original draft, Visualization, Validation, Methodology, Investigation, Formal analysis, Data curation. **Krit Somnuk:** Writing – review & editing, Validation, Supervision, Project administration, Funding acquisition, Conceptualization.

Declaration of competing interest

The authors declare that they have no known competing financial interests or personal relationships that could have appeared to influence the work reported in this paper.

Acknowledgements

This research project was supported by the National Research Council of Thailand (NRCT) (Contract No. N41A650121) and the National Science, Research and Innovation Fund (NSRF) and Prince of Songkla University (Grant No. ENG6701121S).

References

[1] W. Roschat, S. Phewphong, S. Inthachai, K. Donpamee, N. Phudeetip, T. Leelatam, P. Moonsin, S. Katekaew, K. Namwongsa, B. Yoosuk, P. Janetaisong, V. Promarak, A highly efficient and cost-effective liquid biofuel for agricultural diesel engines from ternary blending of distilled Yang-Na (*Dipterocarpus alatus*) oil, waste cooking oil biodiesel, and petroleum diesel oil, Renew. Energ. Focus 48 (2024) 100540, https://doi.org/10.1016/j.ref.2024.100540.

[2] M.A.H. Shaah, M.S. Hossain, F.A.S. Allafi, A. Alsaedi, N. Ismail, M.O.A. Kadir, M. I. Ahmad, A review on non-edible oil as a potential feedstock for biodiesel: physicochemical properties and production technologies, RSC Adv. 11 (2021) 25018–25037, https://doi.org/10.1039/D1RA04311K.

[3] P. Juera-Ong, K. Pongraktham, Y.M. Oo, K. Somnuk, Reduction in free fatty acid concentration in sludge palm oil using heterogeneous and homogeneous catalysis: process optimization, and reusable heterogeneous catalysts, Catalysts 12 (2022) 1007, https://doi.org/10.3390/catal12091007.

[4] S.N.B.A. Khadaroo, P. Grassia, D. Gouwanda, J. He, P.E. Poh, Enhancing the biogas production and the treated effluent quality via an alternative palm oil mill effluent (POME) treatment process: integration of thermal pretreatment and dewatering, Biomass Bioenerg. 151 (2021) 106167, https://doi.org/10.1016/j.biombioe.2021.106167.

[5] N.I.H.A. Aziz, M.M. Hanafiah, S.H. Gheewala, H. Ismail, Bioenergy for a cleaner future: a case study of sustainable biogas supply chain in the Malaysian energy sector, Sustainability 12 (2020) 3213, https://doi.org/10.3390/su12083213.

[6] K. Pongraktham, K. Somnuk, Continuous double-step acid catalyzed esterification production of sludge palm oil using 3D-printed rotational hydrodynamic cavitation reactor, Ultrason. Sonochem. 95 (2023) 106374, https://doi.org/10.1016/j.ultsonch.2023.106374.

[7] C. He, Y. Mei, Y. Zhang, L. Liu, P. Li, Z. Zhang, Y. Jing, G. Li, Y. Jiao, Enhanced biodiesel production from diseased swine fat by ultrasound-assisted two-step catalyzed process, Bioresour. Technol. 304 (2020) 123017, https://doi.org/10.1016/j.biortech.2020.123017.

[8] I. Tobío-Pérez, Y.D. Domínguez, L.R. Machín, S. Pohl, M. Lapuerta, R. Piloto-Rodríguez, Biomass-based heterogeneous catalysts for biodiesel production: a comprehensive review, Int. J. Energy Res. 46 (2021) 3782–3809, https://doi.org/10.1002/er.7436.

[9] Y. Zhang, L. Duan, H. Esmaeili, A review on biodiesel production using various heterogeneous nanocatalysts: operation mechanisms and performances, Biomass Bioenerg. 158 (2022) 106356, https://doi.org/10.1016/j.biombioe.2022.106356.

[10] I.M.R. Fattah, H.C. Ong, T.M.I. Mahlia, M. Mofijur, A.S. Silitonga, S.M.A. Rahman, A. Ahmad, State of the art of catalysts for biodiesel production, Front. Energy Res. 8 (2020) 101, https://doi.org/10.3389/fenrg.2020.00101.

[11] Y.S. Erchamo, T.T. Mamo, G.A. Workneh, Y.S. Mekonnen, Improved biodiesel production from waste cooking oil with mixed methanol–ethanol using enhanced eggshell-derived CaO nano-catalyst, Sci. Rep. 11 (2021) 6708, https://doi.org/10.1038/s41598-021-86062-z.

[12] J. Goli, P. Mondal, O. Sahu, Development of heterogeneous alkali catalyst from waste chicken eggshell for biodiesel production, Renew. Energy 128 (2018) 142–154, https://doi.org/10.1016/j.renene.2018.05.048.

[13] M. Tabatabaei, M. Aghbashlo, M. Dehhaghi, H.K.S. Panahi, A. Mollahosseini, M. Hosseini, M.M. Soufiyan, Reactor technologies for biodiesel production and processing: a review, Prog. Energy Combust. Sci. 74 (2019) 239–303, https://doi.org/10.1016/j.pecs.2019.06.001.

[14] J.P. Valdés, L. Kahouadji, O.K. Matar, Current advances in liquid–liquid mixing in static mixers: a review, Chem. Eng. Res. Des. 177 (2022) 694–731, https://doi.org/10.1016/j.cherd.2021.11.016.

[15] K. Pongraktham, K. Somnuk, Effects of static mixers on continuous methyl ester production: comparing four types of 3D-printed mixing elements, React. Chem. Eng. 8 (2023) 205–219, https://doi.org/10.1039/D2RE00351A.

[16] K. Pongraktham, K. Somnuk, Heterogeneous calcium oxide catalytic filaments for three dimensional printing: preparation, characterization, and use in methyl ester production, ACS Omega 9 (2024) 27578–27591, https://doi.org/10.1021/acsomega.4c03063.

[17] A.M. Díez, F.C. Moreira, B.A. Marinho, J.C.A. Espíndola, L.O. Paulista, M. A. Sanromán, M. Pazos, R.A.R. Boaventura, V.J.P. Vilar, A step forward in heterogeneous photocatalysis: process intensification by using a static mixer as catalyst support, Chem. Eng. J. 343 (2018) 597–606, https://doi.org/10.1016/j.cej.2018.03.041.

[18] R. Lebl, Y. Zhu, D. Ng, C.H. Hornung, D. Cantillo, C.O. Kappe, Scalable continuous flow hydrogenations using Pd/Al_2O_3-coated rectangular cross-section 3D-printed static mixers, Catal. Today 383 (2022) 55–63, https://doi.org/10.1016/j.cattod.2020.07.046.

[19] A. Sharma, P. Kodgire, S.S. Kachhwaha, Investigation of ultrasound-assisted KOH and CaO catalyzed transesterification for biodiesel production from waste cotton-seed cooking oil: process optimization and conversion rate evaluation, J. Clean Prod. 259 (2020) 120982, https://doi.org/10.1016/j.jclepro.2020.120982.

[20] P. Chipurici, A. Vlaicu, I. Calinescu, M. Vinatoru, M. Vasilescu, N.D. Ignat, T. J. Mason, Ultrasonic, hydrodynamic and microwave biodiesel synthesis – a comparative study for continuous process, Ultrason. Sonochem. 57 (2019) 38–47, https://doi.org/10.1016/j.ultsonch.2019.05.011.

[21] R.S. Malani, S. Patil, K. Roy, S. Chakma, A. Goyal, V.S. Moholkar, Mechanistic analysis of ultrasound-assisted biodiesel synthesis with Cu_2O catalyst and mixed oil feedstock using continuous (packed bed) and batch (slurry) reactors, Chem. Eng. Sci. 170 (2017) 743–755, https://doi.org/10.1016/j.ces.2017.03.041.

[22] J. Poosumas, K. Ngaosuwan, A.T. Quitain, S. Assabumrungrat, Role of ultrasonic irradiation on transesterification of palm oil using calcium oxide as a solid base catalyst, Energy Conv. Manag. 120 (2016) 62–70, https://doi.org/10.1016/j.enconman.2016.04.063.

[23] D. Rhithuparna, N. Ghosh, R. Khatoon, S.L. Rokhum, G. Halder, Evaluating the commercial potential of *Cocos nucifera* derived biochar catalyst in biodiesel synthesis from Kanuga oil: optimization, kinetics, thermodynamics, and process cost analysis, Process Saf. Environ. Protect. 183 (2024) 859–874, https://doi.org/10.1016/j.psep.2024.01.030.

[24] K. Somnuk, D. Phanyusoh, J. Thawornprasert, Y.M. Oo, G. Prateepchaikul, Continuous ultrasound-assisted esterification and transesterification of palm fatty acid distillate for ethyl ester production, Processes 9 (2021) 449, https://doi.org/10.3390/pr9030449.

[25] B. Sajjadi, A.A.A. Raman, H. Arandiyan, A comprehensive review on properties of edible and non-edible vegetable oil-based biodiesel: composition, specifications and prediction models, Renew. Sust. Energ. Rev. 63 (2016) 62–92, https://doi.org/10.1016/j.rser.2016.05.035.

[26] Department of Energy Business, Ministry of Energy, Characteristics and quality of fatty acid methyl ester biodiesel. http://elaw.doeb.go.th/document_doeb/TH/690TH_0001.pdf, 2019 (accessed 25 April 2024).

[27] E. Çantı, M. Aydın, Effects of micro particle reinforcement on mechanical properties of 3D printed parts, Rapid Prototyping J. 24 (2018) 171–176, https://doi.org/10.1108/RPJ-06-2016-0095.

[28] M. Khatibi, F. Khorasheh, A. Larimi, Biodiesel production via transesterification of canola oil in the presence of Na–K doped CaO derived from calcined eggshell,

Renew. Energy 163 (2021) 1626–1636, https://doi.org/10.1016/j.renene.2020.10.039.
[29] T. Qu, S. Niu, Z. Gong, K. Han, Y. Wang, C. Lu, Wollastonite decorated with calcium oxide as heterogeneous transesterification catalyst for biodiesel production: optimized by response surface methodology, Renew. Energy 159 (2020) 873–884, https://doi.org/10.1016/j.renene.2020.06.009.
[30] S. Ahmad, S. Chaudhary, V.V. Pathak, R. Kothari, V.V. Tyagi, Optimization of direct transesterification of *Chlorella pyrenoidosa* catalyzed by waste egg shell based heterogenous nano – CaO catalyst, Renew. Energy 160 (2020) 86–97, https://doi.org/10.1016/j.renene.2020.06.010.
[31] P.R. Pandit, M.H. Fulekar, Biodiesel production from microalgal biomass using CaO catalyst synthesized from natural waste material, Renew. Energy 136 (2019) 837–845, https://doi.org/10.1016/j.renene.2019.01.047.
[32] L. di Bitonto, H.E. Reynel-Ávila, D.I. Mendoza-Castillo, A. Bonilla-Petriciolet, C. J. Durán-Valle, C. Pastore, Synthesis and characterization of nanostructured calcium oxides supported onto biochar and their application as catalysts for biodiesel production, Renew. Energy 160 (2020) 52–66, https://doi.org/10.1016/j.renene.2020.06.045.
[33] T. Akter, R. Abdur, M. Shahinuzzaman, M.S. Jamal, M.A. Gafur, S.K. Roy, S. Aziz, M.A.A. Shaikh, M. Hossain, Effect of reaction parameters on CO_2 absorption from biogas using CaO sorbent prepared from waste chicken eggshell, ACS Omega 8 (2023) 43000–43007, https://doi.org/10.1021/acsomega.3c06226.
[34] S. Das, J.M.H. Anal, P. Kalita, L. Saikia, S.L. Rokhum, Process optimization of biodiesel production using waste snail shell as a highly active nanocatalyst, Int. J. Energy Res. 2023 (2023) 6676844, https://doi.org/10.1155/2023/6676844.
[35] A. Attari, A. Abbaszadeh-Mayvan, A. Taghizadeh-Alisaraei, Process optimization of ultrasonic-assisted biodiesel production from waste cooking oil using waste chicken eggshell-derived CaO as a green heterogeneous catalyst, Biomass Bioenerg. 158 (2022) 106357, https://doi.org/10.1016/j.biombioe.2022.106357.
[36] E.E. Çakırca, G.N. Tekin, O. İlgen, A.N. Akın, Catalytic activity of CaO-based catalyst in transesterification of microalgae oil with methanol, Energy Environ. 30 (2019) 176–187, https://doi.org/10.1177/0958305X18787317.
[37] F. Kesserwan, M.N. Ahmad, M. Khalil, H. El-Rassy, Hybrid CaO/Al_2O_3 aerogel as heterogeneous catalyst for biodiesel production, Chem. Eng. J. 385 (2020) 123834, https://doi.org/10.1016/j.cej.2019.123834.
[38] S. Thakur, S. Singh, B. Pal, Superior adsorption removal of dye and high catalytic activity for transesterification reaction displayed by crystalline CaO nanocubes extracted from mollusc shells, Fuel Process. Technol. 213 (2021) 106707, https://doi.org/10.1016/j.fuproc.2020.106707.
[39] Y. Kojima, S. Takai, Transesterification of vegetable oil with methanol using solid base catalyst of calcium oxide under ultrasonication, Chem. Eng. Process. 136 (2019) 101–106, https://doi.org/10.1016/j.cep.2018.12.007.
[40] N. Zhang, H. Xue, R. Hu, The activity and stability of CeO_2@CaO catalysts for the production of biodiesel, RSC Adv. 8 (2018) 32922–32929, https://doi.org/10.1039/C8RA06884D.
[41] A. Gholami, F. Pourfayaz, A. Maleki, Techno-economic assessment of biodiesel production from canola oil through ultrasonic cavitation, Energy Rep. 7 (2021) 266–277, https://doi.org/10.1016/j.egyr.2020.12.022.
[42] T. Wongwuttanasatian, K. Jookjantra, Effect of dual-frequency pulsed ultrasonic excitation and catalyst size for biodiesel production, Renew. Energy 152 (2020) 1220–1226, https://doi.org/10.1016/j.renene.2020.01.149.
[43] K.N. Krishnamurthy, S.N. Sridhara, C.S.A. Kumar, Optimization and kinetic study of biodiesel production from *Hydnocarpus wightiana* oil and dairy waste scum using snail shell CaO nano catalyst, Renew. Energy 146 (2020) 280–296, https://doi.org/10.1016/j.renene.2019.06.161.
[44] A.R. Gupta, S.V. Yadav, V.K. Rathod, Enhancement in biodiesel production using waste cooking oil and calcium diglyceroxide as a heterogeneous catalyst in presence of ultrasound, Fuel 158 (2015) 800–806, https://doi.org/10.1016/j.fuel.2015.05.064.